# Research on Synchronization Technology of Dynamic Environment Signals in the Laser Measurement and Control System

Yifan Yang[1], Yujie Lin[1], Yuting Zhang[2], Chunyuan Hu[1], and Jie Zeng[2](✉)

[1] School of Information and Electronics, Beijing Institute of Technology, Beijing 100081, China
{3220230923,linyujie,chunyuanhu}@bit.edu.cn

[2] School of Cyberspace Science, Beijing Institute of Technology, Beijing 100081, China
{1120200732,zengjie}@bit.edu.cn

**Abstract.** With the development of deep space exploration technology, space laser communication technology has been paid more attention to, and communication and ranging are increasingly integrated. Pulse position modulation (PPM) is more suitable for deep space exploration in many ways. The key and difficulty of the performance of the laser measurement and control system lie in the high-precision synchronization algorithm of the signal. This paper mainly studies the PPM synchronization technology in the laser measurement and control system, which is expected to realize the accurate ranging with low synchronization accuracy under a high dynamic environment. We study the basic framework of laser measurement and control system and the ranging principle. The reason why PPM modulation is chosen to realize the synchronization algorithm is also analyzed. Then, we focus on the capture algorithm based on sliding correlation and the digital delay locking loop tracking algorithm, and design the phase discrimination frequency gain Kv to improve the sensitivity of the loop to first-order dynamics. Finally, the simulation results show that under the input condition of 16-ppm modulation mode, the time synchronization accuracy can meet the requirement of less than 100 ps in the dynamic range of 2000 m/s. Therefore, this technology is of great significance for the development of aerospace, deep space exploration and other fields in the future.

**Keywords:** Laser measurement and control system · Laser ranging · Pulse Position Modulation · Signal synchronization

This work was supported by the National Key Research and Development Program under Grant 308, the National Natural Science Foundation of China under grant 62001264, the Fundamental Research Funds for the Central Universities, and the Beijing Institute of Technology Research Fund Program for Young Scholars.


F. Gao et al. (Eds.): Chinacom 2023, LNICST 590, pp. 263–279, 2024.
https://doi.org/10.1007/978-3-031-67162-3_17

# 1 Introduction

## 1.1 Research Background

With the development of deep space exploration technology, in order to meet the needs of large information capacity and high dynamic transmission, the working style with only the traditional electromagnetic wave technology is no longer effective in the radio frequency band. And space laser communication technology is getting more and more attention because of its strong communication ability [1], low efficiency and good confidentiality characteristics, while laser in ranging has also shown the advantages of high accuracy, short measurement time, communication and ranging began to develop toward the direction of integration. Among many laser modulation methods, pulse position modulation (PPM) has the advantages of large communication bandwidth, good confidentiality, simple coding, etc., and is suitable for deep space detection [2]. Therefore, the research on PPM Modulation and demodulation technology of laser measurement and control system are of great significance.

The key and difficulty of laser measurement and control system performance lies in the high-precision synchronization algorithm of the signal [3]. The synchronization algorithm includes two parts: capture and tracking, the former aims to find the required information from the transmitted signal. The latter aims to complete the accurate synchronization of the signal. And the synchronization information will be used for communication demodulation and ranging. Synchronization algorithm is the core of laser measurement and control integrated system. In addition, the development of military, aerospace, measurement and other technologies has made more and more occasions, such as the installation of large-scale experimental equipment, deep space communication, etc., have a demand for large-scale, high-precision, fast and dynamic distance measurement, which makes it more important to achieve accurate signal synchronization in a high-dynamic environment. Especially in the high dynamic environment, due to the relative motion between objects to produce the Doppler effect, change the transmission speed of the signal, so in this case, maintaining the accuracy of the signal synchronization is also the key and the hardest part [4].

In terms of signal acquisition technology, G.F. Sage [5] first proposed the sliding correlation serial acquisition method of pseudorandom signals, which determines the synchronization time by linearly changing the time difference between the local pseudo-code sequence and the received sequence and making continuous decisions. R.B. Ward [6] proposed the capture method of sequential detection, which needs to determine the seed value of the pseudorandom sequence before demodulation, and then recursively generate local pseudorandom code, which has the characteristics of simple structure and fast capture speed. For the signal tracking algorithm in high dynamic environment, with continuous development, phase-locked loop related technology with low difficulty of implementation has been more and more advanced and has become the most common method. For example, Navicom R.D Center in South Korea has studied the HDGPSR that can change the loop mode under different dynamic environments [7]. In high dynamic environments, it is the mode of frequency-locked loop assisted PLL, while in low dynamic environments, it is the PLL operating mode.

### 1.2 Main Contributions

This paper mainly studies the structure of the laser measurement and control system, as well as the basic principle of PPM modulation and ranging. Then we use sliding correlation capture and digital delay lock loop tracking algorithm to achieve PPM signal synchronization, and finally reaches the target requirements through simulation experiments. The key contributions of this paper are summarized as follows.

- The basic structure of the laser measurement and control system is described, the principle of laser distance measurement and signal synchronization acquisition and tracking algorithm are introduced, and a digital time-delay lock ring with variable parameters is analyzed and designed.
- In order to improve the sensitivity of the loop to first-order dynamics, a phase detection frequency gain $K_v$ loop filter is designed to improve the tracking loop to maintain both faster tracking speed and higher tracking accuracy.
- Through comparison experiment, distance measurement simulation is carried out in different dynamic environments, and the target requirement of time synchronization accuracy less than 100 ps in the dynamic range of 2000 m/s is achieved, and the accurate distance measurement is completed.

### 1.3 Organization

The remainder of this paper is organized as follows. In Sect. 2, the system model for laser measurement and control system and the basic principle of asynchronous response ranging in laser ranging mode are described. In Sect. 3, the process and performance of PPM synchronization are analyzed, with emphasis on the sliding correlation acquisition algorithm and digital delay locking loop tracking algorithm, and the improved method is proposed. Simulation results and corresponding analysts are given in Sect. 4, followed by the conclusions in Sect. 5.

## 2 System Model and Basic Principle

The laser measurement and control system combines the function of digital communication with the function of high-precision time measurement to form an integrated system. The accurate distance measurement can be completed at the same time of receiving the signal, which has a good application prospect.

According to the different functions, the laser measurement and control system can be roughly divided into two parts: the main test end and the tested end. In the real scene, the main measuring end is the ground station, and the measured end represents the satellite. In the data link, the uplink is the main test end to transmit signals to the tested end, and the opposite is the downlink transmitted from the tested end to the main test end [8]. The transmission rate of the uplink is much smaller than that of the downlink, so it is asymmetrical. The overall block diagram of the system is shown in Fig. 1.

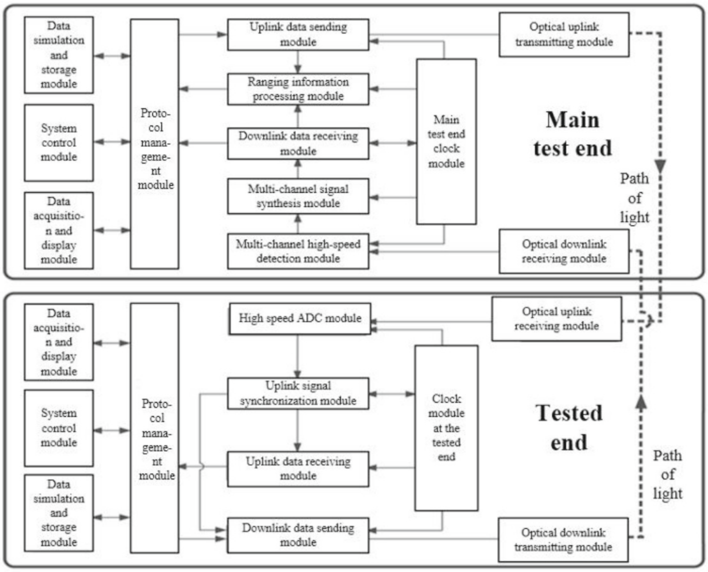


**Fig. 1.** Functional block diagram of integrated laser communication ranging system.

In laser ranging technology, there are three operating modes: asynchronous response, symbol count and synchronous forwarding. This paper adopts asynchronous response ranging, which belongs to a non-coherent ranging method, and the uplink and downlink data are independent of each other. This method can greatly improve the measured distance, and can obtain the time difference between the ground station and the satellite information. The principle is illustrated in Fig. 2.

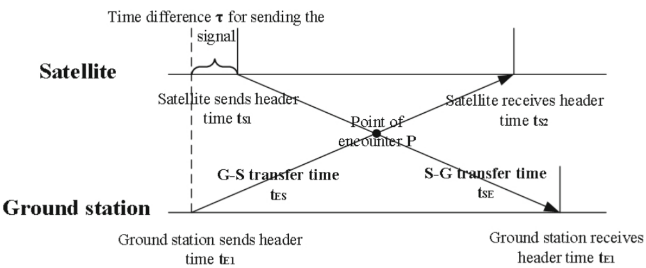


**Fig. 2.** Principle of asynchronous reply ranging.

In this process, the satellite and the ground station each refer to their local clock system and send the distance measurement frame data to the other side at the same frequency, and then respectively measure the time difference between the moment of their own transmission of the distance signal and the moment of receiving the signal transmitted by the other side. The time difference between the ground station and the satellite signal $\tau$ can be obtained by Eq. (1).

$$\tau = (t_{E2} - t_{E1}) - t_{SE} \tag{1}$$

where $t_{SE}$ represents the transmission time of the signal from the satellite to the ground station, and the distance between the star and the ground can be obtained by multiplying the speed of light c. $t_{SE}$ and $t_{SE}$ are measured at ground stations. In this way, the clock difference between the stars and the ground is obtained, and the basic conditions for the time synchronization between the stars and the ground are provided.

# 3 Performance Analysis

## 3.1 PPM Modulation

First proposed by Pierce J R, PPM modulation is a way of representing data by the relative position of the pulse in the time slot in a symbolic period. In pulse position modulation, a symbol is divided into multiple time slots, and the pulse appearing in different time slot positions represents different information.

If the n-bit data set is written as $M = (m_n, m_{n-1}, ......, m_1)$ and the slot position is written as L, the encoding mapping of this L-ppm is as follows:

$$l(M) = m_1 + 2m_2 + ...... + 2^{n-1}m_n \tag{2}$$

A partial diagram of 16-PPM can be obtained, as shown in Fig. 3.

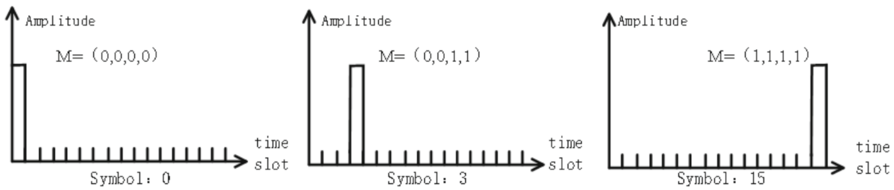


**Fig. 3.** Schematic diagram of 16-PPM.

In addition, if the pulse amplitude of L-PPM modulation mode is assumed to be P, the average transmitted power per code element is P/L. For OOK modulation mode, assuming that the power when transmitting signal 1 is P, and the probability of transmitting signal 1 and transmitting signal 0 are the same, that is, 0.5, the average power of OOK is P/2, so the transmission power of PPM mode is smaller than that of OOK mode, which can improve efficiency and save energy [9,10].

### 3.2 Sliding Correlation Acquisition Algorithm

The capture process is to roughly estimate the moment of the current signal, it can use less prior information to quickly search the initial phase of the synchronization code. But the synchronization accuracy is limited, and can be mainly divided into serial capture and parallel capture. By constantly adjusting the phase of the local code, it correlates and integrates with the received signal in real-time. Because the correlation peak is generated only when the code sequence is exactly aligned, the correlation results can be used for threshold judgment to judge whether the capture is successful.

The most commonly used sliding-correlation acquisition algorithm is a single integral acquisition, which is simple in structure and consumes less resources, but its acquisition time is longer, so it is more suitable for low-speed serial data transmission and non-fast acquisition application scenarios. Figure 4 shows the working principle.

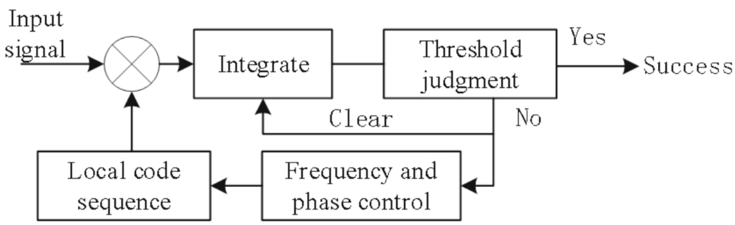


**Fig. 4.** Schematic diagram of single integral sliding correlation.

The PPM source data information is continuously transmitted by time division multiplexing (TDM) after framing (Fig. 5).

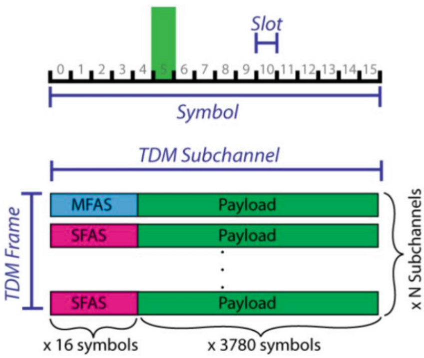


**Fig. 5.** TDM frame data format.

The frame format of PPM signal is that each frame data includes 3796 PPM symbols, of which the first 16 symbols are fixed frame header synchronization codes for PPM signal capture and tracking, and the last 3780 symbols are encoded frame data. Each PPM symbol can be mapped into 16 time slots, and each time slot represents 1bit of transmitted information, so each frame contains 60,736 fixed time slots and data bits.

The system is used to synchronize the sequence "Ox 41C1 D5B7 A0DE 18DF" with 256 time slots as the head of the selected ranging frame. The autocorrelation curve of the synchronization code can be obtained by periodic autocorrelation operation, as shown in Fig. 6.

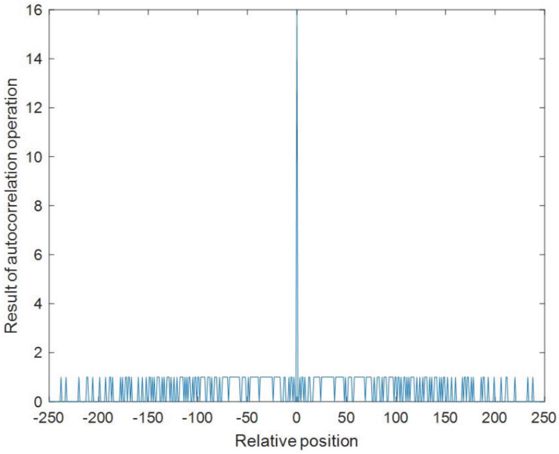


**Fig. 6.** PPM frame head sequence autocorrelation function.

The figure shows that the correlation result has only one highest value, which is calculated when the two frame headers completely coincide, and the correlation value reaches 16. It can be seen that the frame synchronization code has good autocorrelation characteristics, and its maximum correlation result is much larger than other relative positions. Therefore, the system selects the sliding correlation algorithm for acquisition and can basically estimate the signal reception time.

The operation process can be expressed by Eq. (3).

$$Z(n) = \frac{1}{N}\sum_{m=0}^{N-1} x(m)y(n-m) \tag{3}$$

where $x$ is the local synchronization sequence, y is the received signal, n is the relative delay of the local synchronization sequence and the received sequence, $z(n)$ is the correlation value of the local synchronization code and the received signal under the current delay, $z(n)$ reaches the maximum value when the two are completely aligned, where the arrival time of the received signal is $n$.

### 3.3 Variable-Parameter Digital Delay Lock Loop

After the acquisition, the phase difference between the received signal and the local signal has been basically kept within the synchronization range. In order to improve the demodulation quality and the ranging accuracy, it is also necessary to use the digital delay locking loop to track the signal and restore the signal phase (time) in the local area, so that the received code and the local code can automatically and continuously maintain high precision phase alignment. In order to achieve more accurate synchronization.

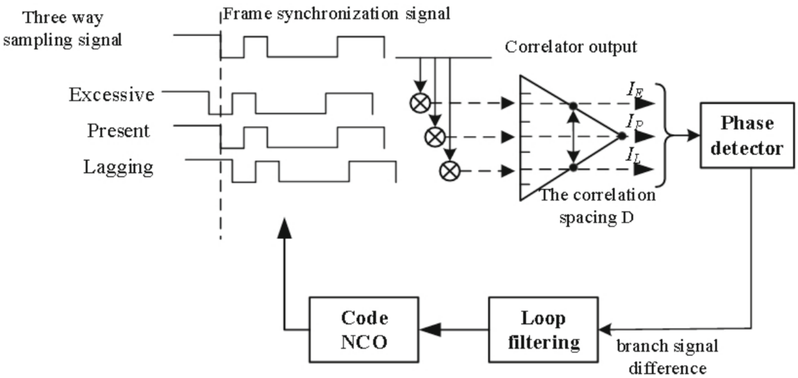


**Fig. 7.** Schematic of the digital delay-locked loop.

According to the function, the digital delay-locked loop can be mainly divided into four parts, which are integral clearance, phase discrimination, loop filtering and code numerically controlled oscillator(NCO). The basic principle is shown in Fig. 7.

When the frame synchronization code is successfully captured by the receiver, it is copied into the same three copies, which are correlated with the local three excessive, present and lagging synchronization code signals respectively, that is, the integral clearance process, and the results are input into the phase discriminator to compare the obtained phase difference, that is, the time difference. Then it is input to the code NCO module through loop filtering, and the local synchronization code is adjusted to generate the next time, and the above process is repeated. Finally, through continuous feedback and adjustment, the frequency and phase of the locally generated synchronization code can be consistent with that of the frame synchronization code sampled by the receiver, and the delay value of the received signal can be obtained. The process is as follows.

**Integral Clearance.** Integral clearing simultaneously correlated the received sampled signal with three local synchronization codes to determine the phase difference (Fig. 8).

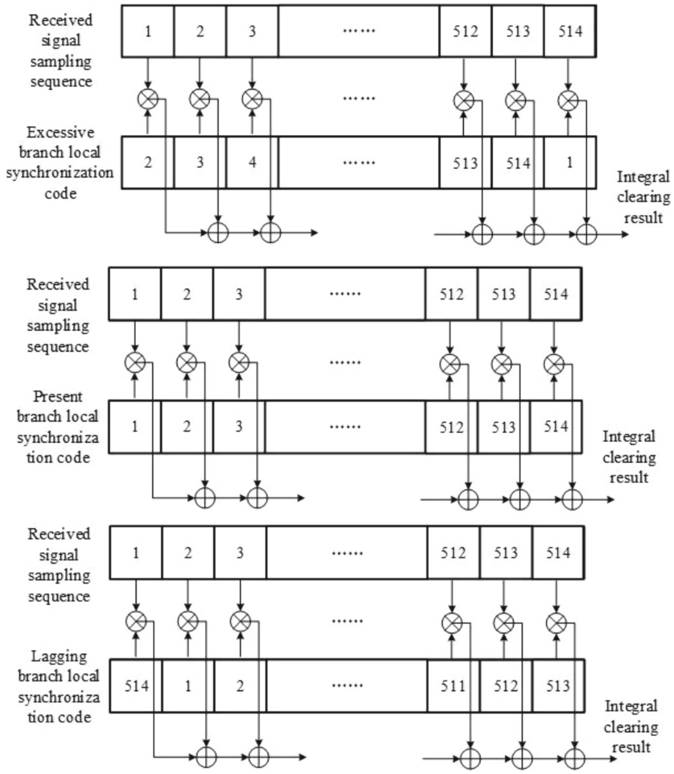


**Fig. 8.** The three-way local code integration process.

The local synchronization code sampled by the estimated frequency and phase information is the instant code, and its branch is the present branch P. The local synchronization code whose phase is ahead of the instant code is the lead code, and the branch is the excessive branch E. The local synchronization code whose phase lags behind the instant code is the lagged code, and the branch in which it is located is the lagging branch L.

The three-way integration results are IE, IP and IL, respectively, and the integration process is shown in Fig. 9. Only when the receiving code is aligned with the synchronization code, the integral clearing result is all positive, which will be the largest.

**Phase Discrimination.** The role of the digital phase discriminator is to detect the phase difference value between the local synchronization code and the received code, which is the feedback variable of the digital signal tracking loop.

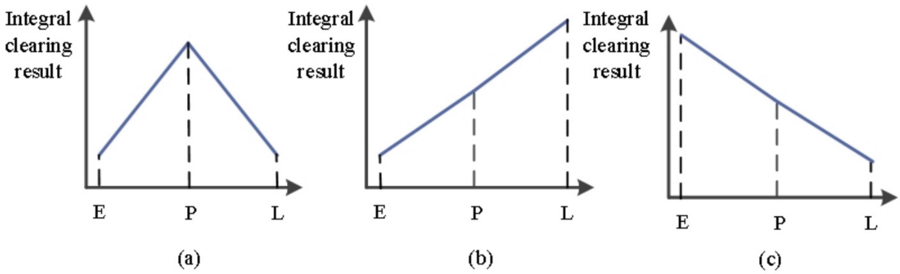


**Fig. 9.** Three-way integral clearing result. (a) just aligned (b) the receiving code lags behind the local synchronization code (c) the receiving code is ahead of the local synchronization code

As shown in Fig. 9, (a) is just aligned; (b) needs to adjust the local code backward; (c) needs to adjust the local code forward.

After obtaining IE and IL, the normalized lead minus lag amplitude method is used for phase detection, and the phase detection formula is

$$e_{ck} = \frac{I_E - I_L}{I_E + I_L} \tag{4}$$

where $e_{ck}$ is the normalized phase difference; when the tracking loop is in a stable state, $I_E$ and $I_L$ are basically equal; at this time, the local synchronization code and the received synchronization code are exactly in the same frequency and phase, $e_{ck} = 0$, otherwise, the difference between them is large and the result is not 0.

**Loop Filtering.** The purpose of loop filtering is to eliminate the interference of noise and extract the dynamic information of the received signal, such as phase and frequency contained in the normalized phase discrimination error. Since the system is under dynamic environmental conditions, the second-order Jaffe-Rechtin digital filter is used in this paper, and Fig. 10 shows its digital form structure.

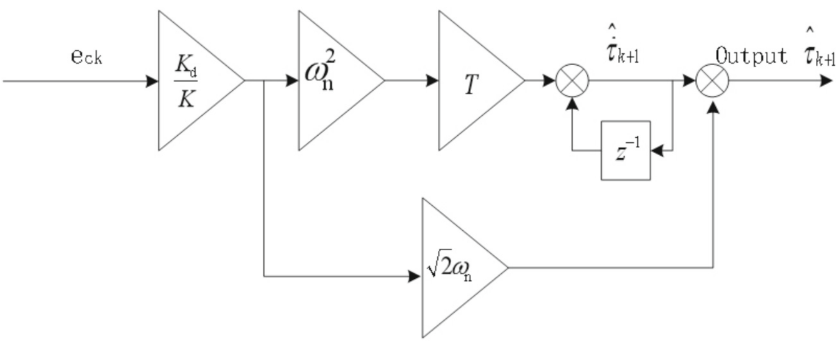


**Fig. 10.** Second-order Jafe-Rechtin digital filter structure.

The recurrence formula of its filtering algorithm can be obtained as

$$\begin{cases} \hat{\dot{\tau}}_{k+1} = \hat{\dot{\tau}}_k + \frac{K_d}{K} e_{ck} \omega_n^2 T \\ \hat{\tau}_{k+1} = (\hat{\tau}_k + \hat{\dot{\tau}}_{k+1}) + \sqrt{2} \frac{K_d}{K} e_{ck} \omega_n T \end{cases} \tag{5}$$

where $\hat{\dot{\tau}}_k$ is the phase estimation of the KTH synchronization code, $T$ is the input update time of the loop filter, and $\omega_n$ is the natural angular frequency of the loop filter. According to the relationship between the second-order loop bandwidth and the angular frequency, $\omega_n = 1.89 B_L$, where $B_L$ is the filter bandwidth, which is an important parameter of the tracking loop.

The size of the loop bandwidth determines how much noise will enter the loop. When the bandwidth is large, the locking speed of the loop is faster, but it is easy to lead to the instability of the loop. When the bandwidth is small, less noise is introduced and the filtering effect is good, but the locking time is long and it may even lose the lock. Therefore, in the choice of bandwidth, not only the adjustment speed should be considered, but also the stability should be considered to ensure that the result is more reasonable.

Therefore, it is often necessary to adjust the bandwidth in the actual dynamic environment. When the receiver completes signal acquisition and is about to enter the tracking algorithm, a large loop bandwidth should be selected to ensure that the loop locks quickly. When the receiver has been locked for N times, the loop is judged to be locked, and the loop bandwidth can be adjusted to reduce the bandwidth appropriately for more accurate adjustment. Until the loop bandwidth is reduced to $B_{L\_stable}$, the loop bandwidth is no longer changed and the stable operation phase is entered. In order to make the tracking loop maintain faster tracking speed and higher tracking accuracy at the same time, the phase discrimination frequency gain $K_v$ can be increased, which only exists in the branch where the frequency parameter is estimated, and the sensitivity of the loop to the first-order dynamics can be improved. The improved loop filter structure is shown in Fig. 11.

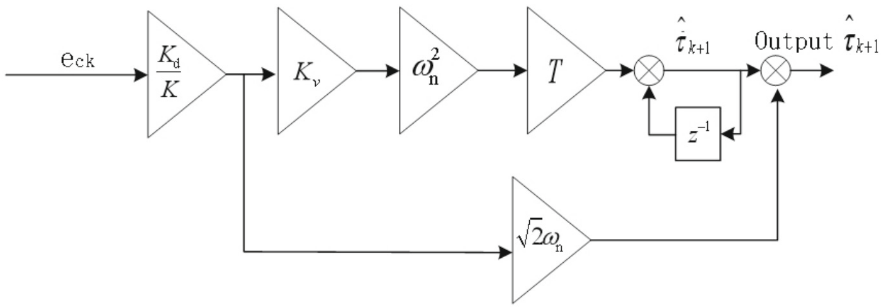


**Fig. 11.** The improved loop filter structure.

The loop filter ultimately produces the code frequency word adjustment increment $\Delta P_{k+1}$ by the formula

$$\Delta P_{k+1} = \frac{\hat{\tau}_{k+1} - \hat{\tau}_k}{2\pi T} K_f \tag{6}$$

where the frequency word conversion factor $K_f = L_f / f_s$, $L_f = 60736$ time slots, fs is the sampling rate. The frequency word increment $\Delta P_{k+1}$ and the initial value $P_{ini}$ of the frequency word set according to the nominal transmission frequency of the signal are accumulated and quantized to form the frequency control word FTW, which is input to the code NCO module.

**Code NCO.** According to the code rate control word (FTW) generated by loop filtering, the code NCO uses a CNC oscillator to generate three new receiver local synchronization codes (excessive, present, lagging) for the next integral clearance. The phase accumulator of NCO will increase FTW at each clock, and it will accumulate until it reaches the limit value and then overflow to zero, and the synchronization code of one cycle will complete the output.

# 4 Simulation Results and Analysis

## 4.1 Capture Algorithm

The dynamic environment is reflected by the relative movement speed of the transceiver system. The relative motion between objects produces Doppler effect and changes the transmission speed of the signal. According to the Doppler frequency offset formula (7), the radial velocity v of the satellite determines the size of the transmission rate change $\Delta R_b$.

$$\Delta R_b = \frac{v}{c} R_b \tag{7}$$

The simulation is done using MATLAB, the channel model is an AWGN channel, and a random distance value is set at the transmitter as a random delay in the system. Since the phase offset can reduce the normalized correlation peak, the fixed decision threshold is set to about 75% of the correlation peak, and the detection probability when EbN0 is 3 dB, 5 dB, 8 dB, 11 dB and 14 dB is simulated respectively. The single decision, the simulation times are 10000, and different relative speeds are set.

The simulation results are shown in Fig. 12.

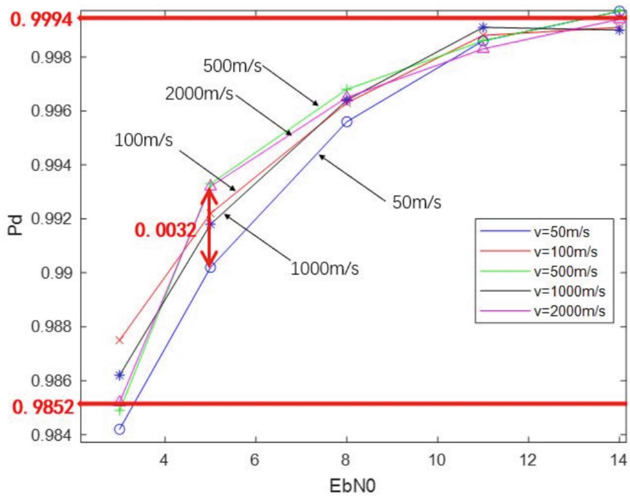


**Fig. 12.** Detection probability as a function of EbN0 and speed.

From the simulation results in dynamic environment, the detection probability increases with the increase of EbN0. And it can be seen that the detection probability changes little when the speed increases, and the maximum difference is only 0.32%, which is basically not affected by the dynamics. Since the (dynamic) speed required in the system index is less than 2000 m/s, the detection probability reaches more than 98% even when EbN0 = 3 dB at the maximum speed, which indicates that the acquisition algorithm can meet the needs of the system.

## 4.2 Tracking Algorithm

According to the design index requirements, dynamic simulation experiments are carried out, and the simulation parameters are shown in Table 1.

**Table 1.** Simulation parameters of dynamic environment tracking algorithm

| Index | Value |
|---|---|
| $R_{slot}$ | 311.04 Mslot/s |
| modulation system | 16-PPM |
| $f_s$ | 625 Msps |
| simulation frequency | 500 |
| $K_v$ | 10000(first 100 frames)<br>100(100 to 200 frames)<br>1(after stability) |
| $B_{L\_unstable}$ | 0.06 Hz |
| $B_{L\_stable}$ | 0.02 Hz |

By changing the value of $v$ under dynamic parameters, the influence of $SNR$ on the tracking loop integration results and the normalized phase discrimination error is compared and simulated (Figs. 13 and 14).

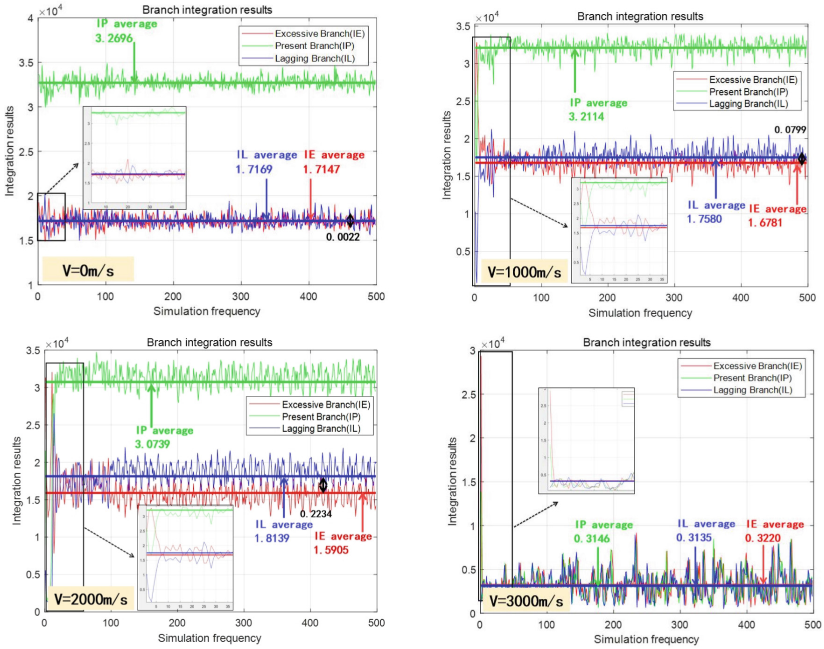


**Fig. 13.** Results of branch integration at different velocities.

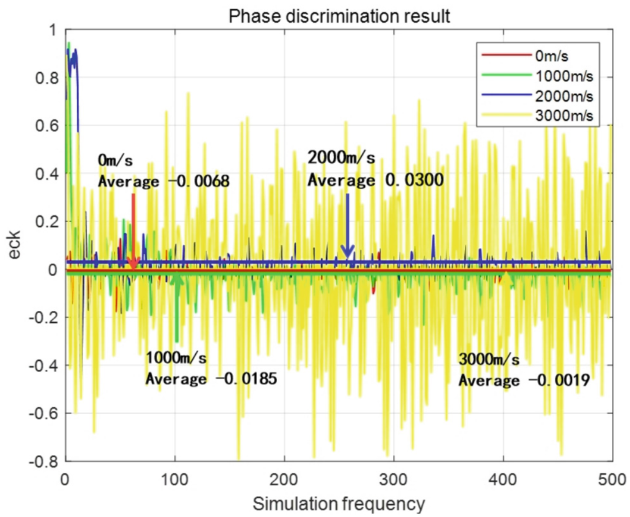


**Fig. 14.** Phase discrimination results at different velocities.

The comparison shows that when the SNR and bandwidth of the loop are the same, the increase of the relative speed of the transmitter and receiver will make the difference between the results of the leading branch and the lagging branch after integral clearance become larger, and the phase discrimination value will not fluctuate around zero value. And with the increase of the relative speed, the adjustment range of the loop becomes larger and the stability of the loop becomes worse, which will cause the loop to lose lock after exceeding a certain speed range.

### 4.3 Distance Measurement Simulation

With the local clock, the phase of the receiver code table is extracted every 27 frames, and the obtained code table phase is subtracted by the frame length, and then the ranging result is obtained by unit conversion. Finally, it was inserted into the data frame and sent to the other party to complete the asynchronous reply ranging. And the simulation parameters are shown in Table 2.

**Table 2.** Simulation parameters of distance measurement

| Index | Value |
|---|---|
| Interval frame number | 27 |
| Frame length | $60736 \times 2^{32}$ |
| Initial distance value | 2057.250576 |
| Range frequency | 18 |

The distance measurements results is shown in Fig. 15.

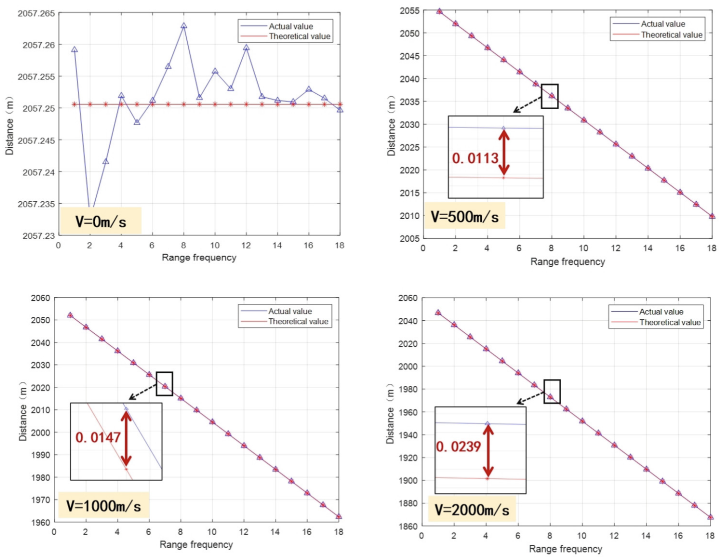


**Fig. 15.** Distance measurements at different velocities.

The distance-measuring error is shown in Fig. 16.

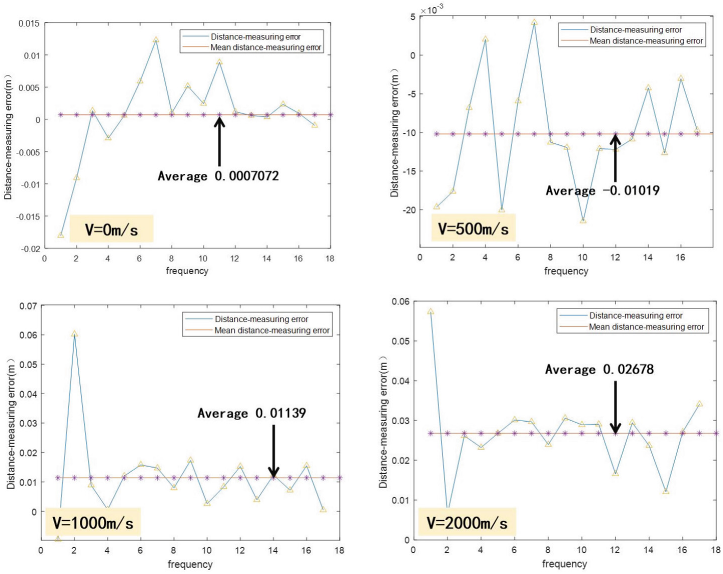


**Fig. 16.** Distance-measuring error at different velocities.

The time synchronization accuracy results are shown in Table 3.

**Table 3.** Time synchronization accuracy at different velocities

| Velocity (m/s) | Time synchronization accuracy (ps) |
|---|---|
| 0 | 28.3698 |
| 500 | 29.6917 |
| 1000 | 33.7210 |
| 2000 | 54.2712 |

It can be seen that with the increase of speed, the average ranging error and time synchronization accuracy increase, but the system can achieve accurate synchronization of PPM signals, complete communication and ranging functions at the same time, and meet the time synchronization accuracy of less than 100 ps (EbN0 = 14 dB) and adapt to the dynamic range of less than 2000 m/s indicators.

## 5 Conclusion

In this paper, we have mainly studied the laser measurement and control system based on PPM modulation, and focused on the PPM signal synchronization technology in dynamic environment. The sliding correlation acquisition algorithm and variable parameter digital delay locking loop have been used to design and improve the system. The simulation results have shown that the system can achieve time synchronization accuracy of less than 100 ps in the dynamic range of 2000 m/s, and achieve the requirements of accurate ranging.

Therefore, the advantages of laser communication ranging integration technology and PPM modulation are becoming more and more obvious in the space field. In the future, the technology will gradually become another new technology in the field of space measurement and control, and continue to expand its application range, to achieve a large range, high precision, fast and dynamic distance measurement in large-scale experimental equipment installation, deep space communication and other scenarios.

## References


1. Li, W.: Research on the trend of laser communication and ranging technique. Laser Infrared **43**(8), 3 (2013)
2. Zhao, W.: Research on synchronization technology of ppm wireless optical communication. Opt. Commun. Technol. **32**(4), 3 (2008)
3. Zaiton, A.M., Eng, C.H., Jasman, F.: Pulse position modulation characterization for indoor visible light communication system. J. Phys. Conf. Ser. **1502**, 012005 (2020)
4. Zhang, W., et al.: Research on simulation methods for doppler frequency shift of a coherent inter-satellite laser link in a ground test system. Infrared Phys. Technol. **113**, 103627 (2021)
5. Sage, G.F.: Serial synchronization of pseudonoise systems. IEEE Trans. Commun. Technol. **12**(4), 123–127 (1965)
6. Ward, R.B.: Acquisition of pseudonoise signals by sequential estimation. IEEE Trans. Commun. Technol. **13**(4), 475–483 (2003)
7. Roncagliolo, P.A., Blasis, C.E.D., Muravchik, C.H.: GPS digital tracking loops design for high dynamic launching vehicles. In: IEEE Ninth International Symposium on Spread Spectrum Techniques Applications (2006)
8. Willis, M.M., Robinson, B.S., Stevens, M.L., Romkey, B.R., Boroson, D.M.: Downlink synchronization for the lunar laser communications demonstration. In: 2011 International Conference on Space Optical Systems and Applications (ICSOS)
9. Jiang, Y., Tao, K., Song, Y., Fu, S.: Packet error rate analysis of OOK, DPIM, and PPM modulation schemes for ground-to-satellite laser uplink communications. Appl. Opt. **53**(7), 1268 (2014)
10. Wu, W.C.: Toward the energy efficiency of multi-pulse ppm signalling for optical communication. IET Commun. **14**(3), 532–538 (2020)